



# Measuring the Hemodynamic Flow in the Brachial-Ulnar-Radial Arterial System

Alexandru M. Morega, Cristina Săvăstru, and Mihaela Morega

## Abstract

Cardiovascular investigations start with the arterial blood pressure measurement and the easiest and accessible approach takes the recording of the systolic and diastolic pressure levels by a sphygmomanometer, usually during compression of the upper arm, or the wrist (same level as the heart), on the path of the brachial artery. More information on arterial hemodynamic, beyond blood pressure monitoring, could result from investigations based on the pulse wave analysis, like applanation tonometry, which is based on pressure sensed on the arm's surface, at several observation points along the brachial tree.

The reactivity and the accuracy of the sensors depend on their design; capacitive and piezoelectric sensors are good candidates for this task. Based on numerical analysis, the work presented here evaluates the usage of applanation tonometry data for the investigation of hemodynamic parameters and examines some technical and medical aspects of the method. The multiphysics numerical model assembles three different problems: hemodynamic flow, structural deformation of the arm and generation of electricity through deformable sensors.

## 1 Introduction

Blood pressure measurement represents the elementary cardiovascular investigation; it commonly is the fast output of a noninvasive test performed at

---

Key Words: blood pressure; radial applanation tonometry; arterial hemodynamic; piezoelectric pressure transducer; numerical simulation; finite element.

2010 Mathematics Subject Classification: Primary 92C50, 74F10, 74F15; Secondary 65M99, 76M99.

Received: December, 2014

Revised: January, 2015

Accepted: March, 2015

the brachial artery level and gives basic information on the cardio-circulatory system condition [1],[2]. Blood pressure monitoring techniques use pressure transducers, which are sensitive to changes in the arterial flow, enhanced by local compression; they record deformations of the arterial wall [3],[4],[5]. The brachial artery is a preferred location for the measurement because its anatomical and circulatory positions are proximal to the aorta, providing good correlation with the cardiac rate; its path goes close to the skin, where the sensors for measurements in the arterial circulatory system are placed [6],[7].

Recent studies suggest that the central blood pressure is more significant and rich in information than the peripheral pressure, although the last one is much easier obtained, and measurement techniques based on pulse wave analysis provide data on hemodynamic parameters, useful for the cardiovascular diagnostic [8],[9].

In line with these remarks, *Applanation Tonometry* (AP) is a method measuring the force needed for the compression of a given elastic surface, to determine the internal pressure; it comes from oculometry (measurement of the intraocular pressure), but its extension to blood pressure estimation, especially applied at the brachial bifurcation, already proved proficient [4],[10],[11].

An array of pressure sensors is distributed on the arm's surface and simultaneous signal recordings are performed. The reactivity and accuracy of the sensors depend on their design; capacitive [12]-[14] and piezoelectric transducers (PZTs) [15] are good candidates for this task. Several sensors are spread on the arm, along the brachial-radial-ulnar tree; they are secured with a cuff, which applanates the surface of the skin against which they are pressed.

Due to fixation and firm contact, the pressure wave that propagates through the arterial wall and the tissue layers (muscle, fat, skin) is sensed through the change in the sensors' state; PZTs generate electrical signals proportional to their deformation, while capacitive sensors modify their electric parameters (capacitance and resistance). This work is concerned with the PZTs.

One could represent the whole arm through a transfer function between the blood pressure and electrical responses [9],[12],[13]. In this study we simulated the anatomical domain, *i.e.* the arm with its main anatomical structure (bone, muscle and brachial artery), using a medical images based generated model [16], which includes a set of Computer Aided Designed (CAD)[17] PZTs.

The mathematical model integrates three different physical problems: the blood flow dynamics through the artery, the structural deformation of the arm (due to the elasticity of the blood vessel and the muscle) and the piezoelectric conversion of the pending mechanical load into electrical signals.

## 2 A More Realistic Computational Domain

While idealized computational domains [15] are usable, there is a growing interest for more realistic ones that may be obtained, for instance, through image reconstruction techniques [20]. Here, Simpleware [16] was used to process DICOM data sets of computer tomography (CT) scans, aiming to create geometries that represent more accurately the human arm anatomy: the arterial tree, the *humerus*, *radius* and *ulna* bones, the muscular and tissue mass, Fig.1. The gray scale level can be set in the histogram for appropriate rendering, and the available segmentation algorithms, which are used to separate organs and tissues between them, *e.g.*, threshold, floodfill, may be used to single out with controllable threshold and confidence the connected regions growth, Fig.2.

The morphological filters are suitable to relatively rank the pixels order

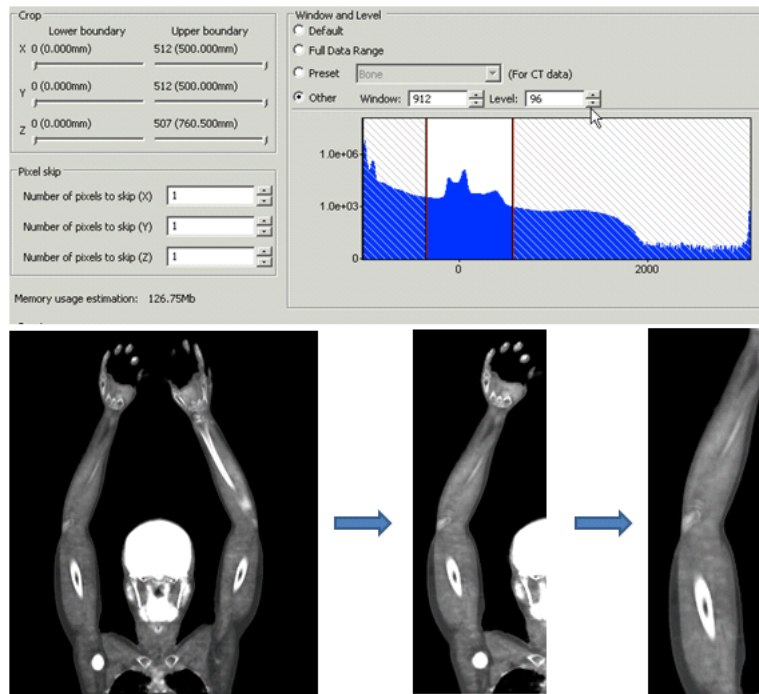


Figure 1: Setting the grey level for a data set [16].

for filling the gaps and preparing the mask for smoothing process. ScanCAD module is then used to build and integrate the sensors with the arm (regroup the masks). Finally, ScanFE [16] produces the finite element (FEM) mesh to

be exported for numerical modeling using [18].

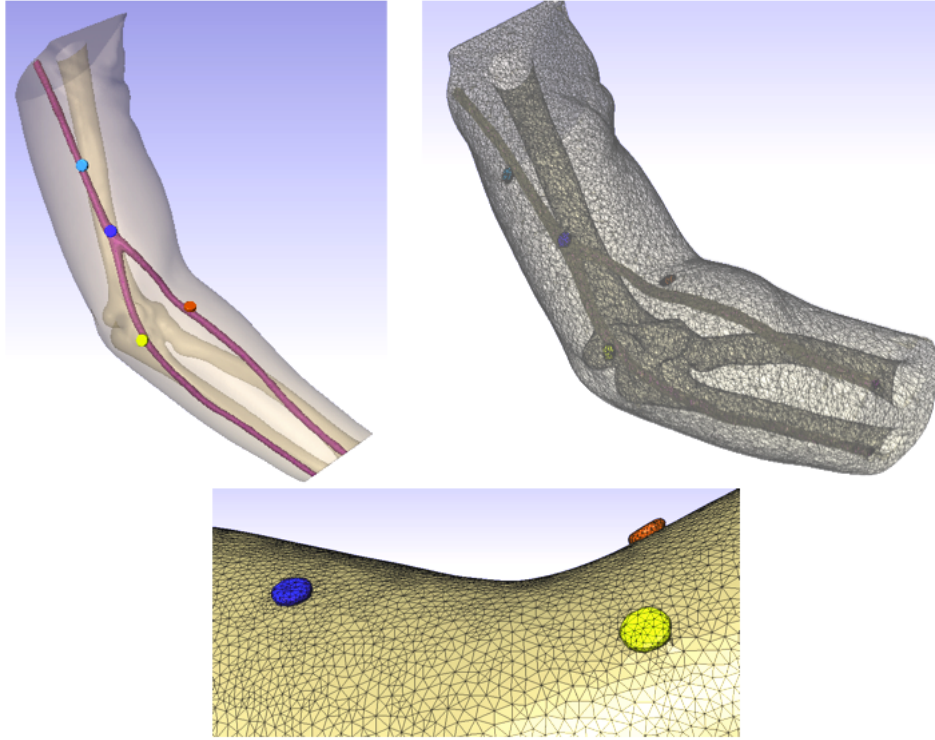


Figure 2: Reconstructed arm [16],[17].

### 3 Numerical Model Description

The computational domain shown in Fig.3 models part of the arm: bones (*humerus, radius, ulna*), the main arteries (*brachial, ulnar, radial*), and the embedding muscular volume.

Assuming that these arterial segment is of “resistive type” [19], the *hemodynamic flow* may be viscous, laminar, incompressible and pulsatile, as described by the momentum balance (Navier-Stokes) and the mass conservation law [20]

$$\rho \left[ \frac{\partial \mathbf{u}}{\partial t} + (\mathbf{u} \cdot \nabla) \mathbf{u} \right] = \nabla \left[ -p \mathbf{I} + \eta \left( \nabla \mathbf{u} + (\nabla \mathbf{u})^T \right) \right], \quad (1)$$

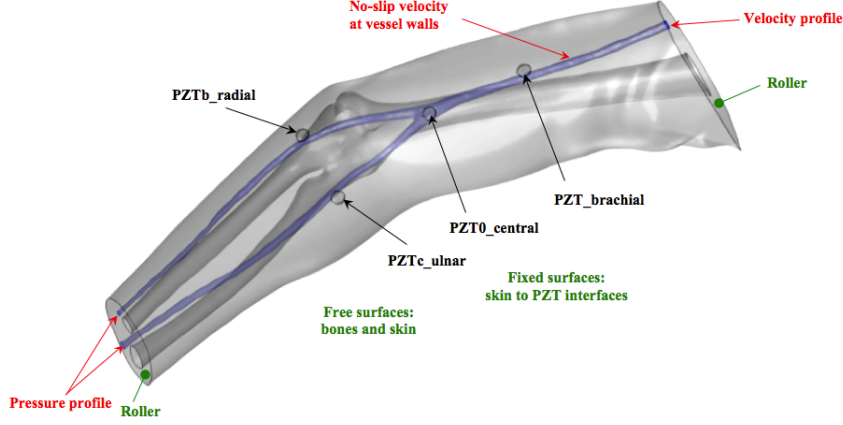


Figure 3: The computational domain and the boundary conditions.

$$\nabla \cdot \mathbf{u} = 0, \quad (2)$$

where  $\mathbf{u}[\frac{m}{s}]$  is the velocity field,  $p[\frac{N}{m^2}]$  is the pressure field,  $\rho = 1,060 \frac{kg}{m^3}$  is the mass density, and  $\eta[Pa \cdot s]$  is the dynamic viscosity. We use the power law type of fluid  $\eta = m\gamma'^{n-1}$  [20], where  $\gamma'[s^{-1}]$  is the shear rate tensor,  $m = 0.017 Pa \cdot s$ , and  $n = 0.708$  are model parameters. This model may solve the discrepancies among published values of the viscosity measured using different techniques [21].

Fig.4 illustrates the velocity boundary condition at the inlet, scaled for the cardiac rhythm of 100 bpm. No-slip velocity conditions are set on the arterial walls. Here, we depart from the previous studies [15],[20], and use for the outlets pressure profiles obtained out of AP measurements, Fig.5.

*The structural model* is solved for the stress generated by the blood flow, determined in the previous step. We assume that the arteries are large enough and pose no resistance to the flow. The bones are a rigid structure with no deformation. However, the musculature and arterial walls are treated as hyperelastic materials [18],[21],[22] - their constitutive law is based on the strain energy density function

$$W = \frac{1}{2} J^{-\frac{2}{3}} \left( I - \frac{1}{3} \bar{I}_1 \right) + \frac{1}{2} \kappa \cdot J (J - 1) C^{-1}, \quad (3)$$

where  $J = \det(\mathbf{F})$  is the relative variation of the volume;  $\mathbf{F}$  is the deformation gradient;  $C = FTF$  is the right Cauchy-Green tensor, and  $\bar{I}_1 = trace(C)$ .

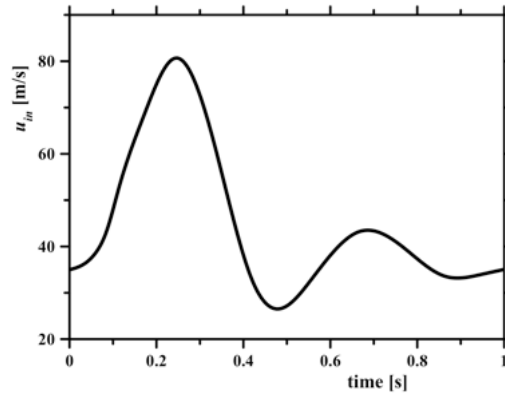


Figure 4: Boundary conditions for the hemodynamic problem.

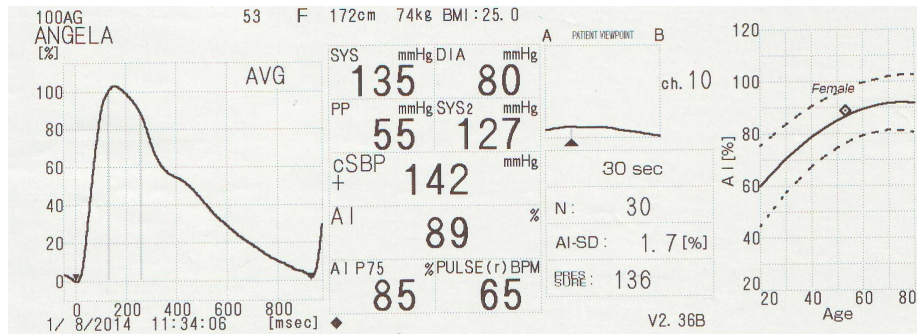


Figure 5: AP measurement data for a healthy, young adult [4],[11].

The initial shear modulus for the muscle is  $\mu = 719,676Pa$  and the initial bulk modulus is  $\kappa = 14,393,520Pa$ , corresponding to Poisson's ratio  $\nu = 0.45$  [21],[22].

The boundary conditions for the two cross-sections of the arm (upper part and forehead) are of "roller" type. The stress upon the vessels walls, an output of the hemodynamic problem, is used as boundary condition (load) in the structural analysis of the deformations of arterial walls produced by pulsatile flow.

The *PZT model* is based on the stress-charge form of the piezoelectric conversion equations

$$\sigma = c_E \varepsilon - e^T \mathbf{E}, \mathbf{D} = e \varepsilon + \varepsilon_0 \varepsilon_{rS} \mathbf{E}, \quad (4)$$

where  $\sigma$  [Pa] represents the stress,  $\varepsilon$  is the strain,  $c_E$  [Pa] is the elasticity matrix,  $e$  [ $\frac{C}{m^2}$ ] is the coupling matrix,  $(\cdot)^T$  is the transposition operator,  $\mathbf{E}$  [V/m] is the electric field strength,  $\mathbf{D}$  [ $\frac{C}{m^2}$ ] is the electric flux density (electrical displacement),  $\varepsilon_0 = \frac{1}{4\pi \cdot 9 \cdot 10^9} \frac{F}{m}$  is the electrical permittivity of the free space and  $\varepsilon_{rS}$  is the relative permittivity of the isotropic piezoelectric material. The stress on the interface transducer - skin surface, an output of the structural model, is applied as load to the PZTs. The upper faces of the PZTs are fixed by the cuff, which is assumed rigid.

The three coupled problems are FEM solved [18], in the order in which they were presented. The final result is represented through the output voltage waveforms generated by the PZTs, which are proportional with the blood pressure transmitted through the arterial vessels.

## 4 Numerical Simulation Results

First, of concern is the mechanical to electrical conversion of the PZTs [15]. Here we present their electrical output, and observe that they produce a linear response (voltage) when submitted to loads that compare to the AP measurements. Next, of concern is the blood flow. To solve this problem, we assume a one-way hemodynamic-structural interaction. Of a particular interest is the brachial-ulnar-radial bifurcation area, where higher gradients of pressure, and other flow events caused by the reflected pressure wave are expected. Next, the structural problem is solved for, by assuming hyperelastic properties for the blood vessel and tissue that participate to the structural model together with a strain energy density function. The strain energy density derives from an isotropic model. Based on the load field, the structural model for the blood vessels and the arm can be observed. The PZT operates at the slow pulse rate

of the circulatory system. The active material is elastic, linear, and with small deformations.

#### 4.1 The Pressure Sensor Response

The PZT is loaded with a force that is proportional to the hemodynamic pressure transmitted through the arm, Fig.6, as AP-measured (Fig.5).

The boundary conditions that close the problem (4) are (mechanical): spec-

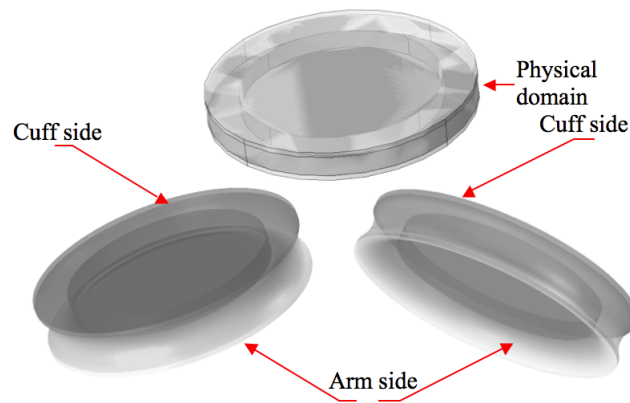


Figure 6: The PZT physical domain (top) and the deformed state (bottom).

ified, normal load for the surface that contacts the skin; the opposite face (by the cuff) is fixed; the lateral side is free, and (electrical): floating potential for the face that contacts the skin; ground for the opposite face (by the cuff); electrical insulation (zero charge density) for the lateral side.

Problem (5) was FEM-solved at different moments during the cardiac cycle. Fig.7 shows the deformation,  $\tilde{\delta}$ , and the output voltage,  $\tilde{V}$ , of the PZT. The two signals are normalized through their maximum values and overlapped, which shows the linear load-voltage response of the PZT. The displacement is presented with circles and the voltage with solid line.

#### 4.2 The Hemodynamic Flow

The brachial-ulnar-radial hemodynamic flow is seen through the velocity field (streamlines, arrows) and deformations in Fig.8 - 0.05s, 0.25s, 0.4s, 1s -

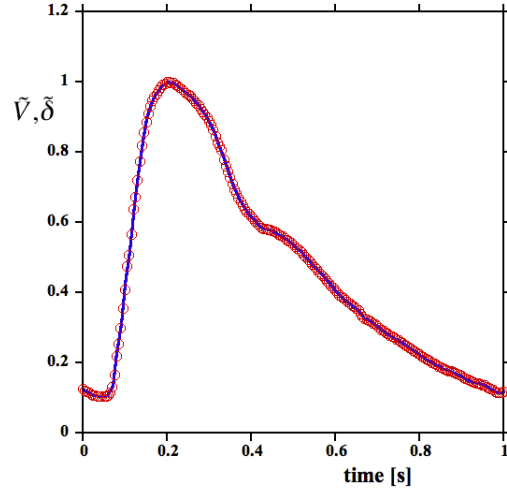


Figure 7: The linear voltage vs. displacement response of the PZT.

thorough arrows (red, velocity) and streamlines (blue, streamfunction). The flow structure, at peak flow rate, shows dynamic recirculation regions in the bifurcation, which is a region of high pressure gradient that suggests higher stresses in the vessels walls. This region, of particular interest in atherosclerosis evolution, makes the object of a vast body of literature [23].

Two major, complex, three dimensional recirculation areas are noticeable in the upstream ulnar and radial arteries entrance regions. Their extension is larger for low flow rate (0,02s, 1s). The recirculation cell in the ulnar section at the maximum flow rate almost vanishes. This bifurcation region is of particular interest in the reflected pressure wave, whose effect is customarily identified in the AP pressure profile [11] ( $t \sim 0.44s$  in Fig.5). Of course, the blood vessel shape plays an important role in the flow structure, but in this study the computational domain (including the arteries) are constructed out CT scans, which makes it closer to real situations.

Fig.9 shows the traction forces that act upon the PZTs. They echo the state of the hemodynamic flow. The largest load is perceived by the central PZT. This could be explained by the local structure of the arm (the supporting bone mass is larger here), to which adds the arterial tree bifurcation that sieges a complex flow which interacts more with the vessels walls - e.g. the rolls that develop in this region.

The early wave ( $t \sim 0.25s$ ) in the brachial artery (Fig.9) is currently as-

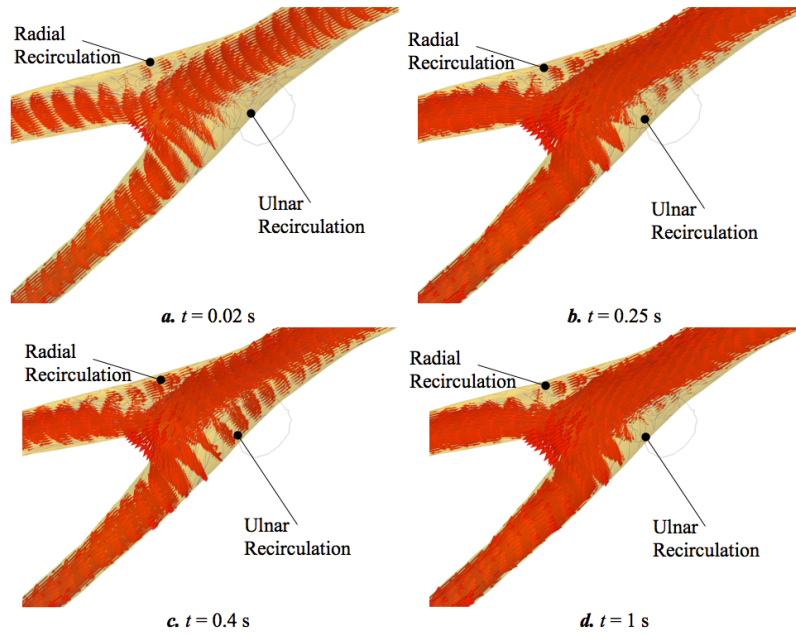


Figure 8: Details of hemodynamic flow in brachial-radial-ulnar bifurcation.

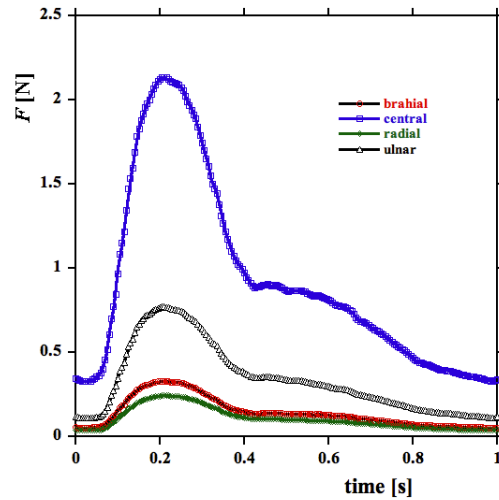


Figure 9: The mechanical loads to the PZTs.

sociated with the fast rise in pressure at the beginning of systole, which is presumably augmented by the reflected compression wave from the bifurcation [6]. The following decay in local pressure ( $t \sim 0.3...0.6s$ ) corresponds to a forward-traveling expansion wave, and the further decay at the end of systole accompanies another forward-traveling expansion wave. Similar pressure dynamics are noticed in radial and ulnar arteries due to the reflected waves produced there by the hand.

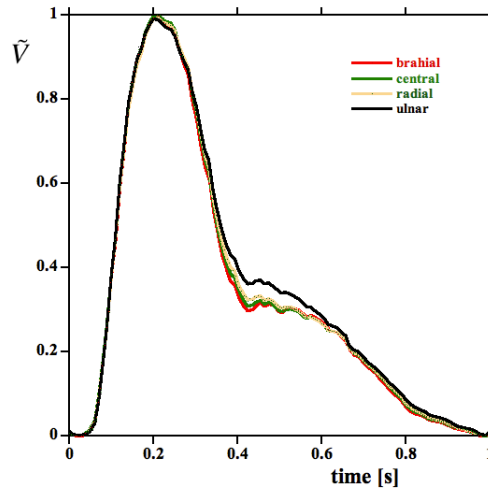


Figure 10: Nondimensional voltages produced by the PZTs.

The PZTs electrical outputs produced by loads generated by the hemodynamic flow are shown in Fig.10 - all PZTs have the same ground reference. The quantities are scaled, using the following definition:  $\tilde{V} = \frac{V - V_{min}}{V_{max} - V_{min}}$ . The maximum and minimum values are listed in Table 1.

**Table 1 - Reference voltages used in scaling PZTs outputs**

<i>Section</i> →	<b>Brahial</b>	<b>Central</b>	<b>Radial</b>	<b>Ulnar</b>
$V_{max}$ [mV]	4.6	330.0	37.8	120.0
$V_{min}$ [mV]	0.72	50.94	5.69	16.99

The profiles overlap, except for the interval  $t \sim 0.3s...0.6s$ , where they differ.

As mentioned before, this interval is thought to correspond to a forward-traveling expansion wave. This departure is more important for the ulnar PZT. It is then interesting to note that the usage of PZTs may be of value in ascertaining such fine details of the hemodynamics that numerical simulations may capture. Further studies will be devoted to these aspects.

## 5 Conclusions

This study was concerned with the pulsatile blood flow in the brachial-ulnar-radial arterial sub-tree, with the aim to understand the usage of appplanation tonometry measurements in relation to blood pressure monitoring, the flow-vessel-muscle structural interactions that occur in the related bifurcation, and to assess the ability of PZTs to sensing of the fine details of the hemodynamic.

The numerical simulations performed using a more realistic computational domain produced through reconstruction techniques and starting from CT scans evidence the complex hemodynamic flow. In particular, the dynamic recirculation cells located by the bifurcation, in the ulnar and radial arteries, are clearly evidenced. They are accompanied by high pressure gradients and deformations, as confirmed by the response of the PZT located above the brachial-radial-ulnar junction. This region may be less exposed to plaque deposition, but the recirculations in the radial and ulnar arteries – more likely favorable for plaque deposition – may menace the bifurcation through vascular fracture.

The pressure wave in the arteries is transmitted through the arm and is sensed by the PZTs. The electrical response of the PZT in this study is linear.

The voltage outputs of the PZTs, properly represented, evidence the discrepancies (shift in time and amplitude) in forward-traveling expansion waves in the three arteries. This departure is more important for the ulnar PZT output. Consequently, the usage of PZTs may be of value in ascertaining such fine details of the hemodynamics that numerical simulations may capture.

**Acknowledgements.** The work was conducted in the Laboratory for Electrical Engineering in Medicine, affiliated with the BIONGTEH platform at UPB. We gratefully acknowledge the support offered by Dr. Mihai CHETAN from MedCo.

## References

- [1] Hiroshi M., "Clinical assessment of central blood pressure," *Curr. Hypertens. Rev.* 2012, DOI: 10.2174/157340212800840708

- [2] Shantanu S., Ghatak An S., *Inexpensive Arterial Pressure Wave Sensor and its application in different physiological condition*, 2005, arXiv:physics/0512071.
- [3] Patvardhan E., Heffernan K.S., et al, *Augmentation Index Derived from Peripheral Arterial Tonometry Correlates with Cardiovascular Risk Factors*, NCBI, 253758, DOI: 10.4061/2011/253758, 2011
- [4] *Non-Invasive Blood Pressure Monitor with Augmentation Index*, HEM 9000AI, Omron.
- [5] DynaPulse Analysis Center <http://www.dynapulse.com/>
- [6] Zambanini A., Cunningham S.L., Parker K.H., Khir A.W., Thom SAMcG, Hughes A.D., "Wave-energy patterns in carotid, brachial, and radial arteries: a noninvasive approach using wave-intensity analysis," *Am. J. Physiol Heart Circ Physiol*, 289, pp. 270–276. 2005.
- [7] Quick C.M., Berger D.S., Noordergraaf A., "Constructive and destructive addition of forward and reflected arterial pulse waves," *Am. J. Physiol Heart Circ. Physiol* 280, pp. 1519–1527, 2001.
- [8] Avolio, A.P., Butlin, M., Walsh, A., "Arterial blood pressure measurement and pulse wave analysis – their role in enhancing cardiovascular assessment," *Physiological Measurement*, 31, R1-R47, 2010.
- [9] Millasseau S.C., Patel S.J., Redwood S.R., Ritter J.M., Chowienczyk P.J., "Pressure wave reflection assessed from the peripheral pulse: is a transfer function necessary," *Hypertension*, 41, pp. 1016–1020, 2003.
- [10] da Fonseca L.J.S., Mota-Gomes M.A., Rabelo L.A., "Radial applanation tonometry as an adjuvant tool in the noninvasive arterial stiffness and blood pressure assessment," *World Journal of Cardiovascular Diseases*, 4, pp. 225-235, 2014.
- [11] Chetan M., "New technologies in blood pressure monitoring," *Proc. of the 8th International Symposium on Advanced Topics in Electrical Engineering (ATEE)*, 23-25 May, 2013, pp. 1-4, DOI:10.1109/ATEE.2013.6563417.
- [12] Ruhhammer J., Ruh D., Foerster K, Heilmann C., Beyersdorf F., Barker A., Jung B., Seifert A., Goldschmidtboeing F., Woias P., "Arterial strain measurement by implantable capacitive sensor without vessel constriction," *Conf. Proc. IEEE Eng. Med. Biol. Soc.* 2012, pp. 535-538. doi: 10.1109/EMBC.2012.6345986.

- [13] Salo T., Kirstein K.U. et al., "Continuous blood pressure monitoring utilizing a CMOS tactile sensor," Conf. Proc. IEEE Eng. Med. Biol. Soc. 2004, 3, pp. 2326-2329.
- [14] Savastru C., Morega A.M., Morega M., "Sensing the Hemodynamic of the Brachial-Ulnar-Radial Arterial System," Proc. of the 8th Intl. Conference and Exposition on Electrical and Power Engineering EPE-2014, Iași, Romania, October 2014, ISBN: 978-1-4799-5848-1.
- [15] Morega A.M., Savastru C., Morega M., "A numerical simulation of the electrical monitoring of the brachial-ulnar-radial arterial hemodynamic," Intl. Conf. on Advancements of Medicine and Health Care through Technology; June 5-7, 2014, Cluj-Napoca, Romania, IFMBE 44, pp. 301-306.
- [16] Simpleware, v.4.2, 2009.
- [17] Solidworks, 2008.
- [18] Comsol Multiphysics, v.3.5a (2010) – v.5.0 (2014).
- [19] Feijóo R.A., *Computational methods in biology*, 2nd Summer School LNCC/MCT, Petrópolis, January 2000.
- [20] Morega A.M., Savastru C., Morega M., "Numerical simulation of flow dynamics in the brachial-ulnar-radial Arterial System," IEEE International Conference on e-Health and Bioengineering, EHB 2013, November 21-23, 2013, Iasi, Romania.
- [21] Elert G., The Physics Hypertextbook-Viscosity. physics.info
- [22] Bangash M.Y.H., Bangash F.N., Bangash T. Trauma, *An Engineering Analysis with Medical Case Studies Investigation*, Springer, ISBN 3-540-36305-X, 2007.
- [23] Deng X., King M., et al., "Localization of atherosclerosis in arterial Junctions," ASAIO Journal, vol. 41, pp. 58–67, 1995. [PubMed: 7727823].

Alexandru M. MOREGA,  
Faculty of Electrical Engineering,  
University POLITEHNICA of Bucharest,  
Splaiul Independenței no. 313, sector 1, 060042 Bucharest, Romania.  
"Gh. Mihoc - C. Iacob" Institute of Statistical Mathematics and Applied  
Mathematics, The Romanian Academy, Romania.  
Email: amm@iem.pub.ro

Cristina SĂVĂSTRU,  
Faculty of Electrical Engineering,  
University POLITEHNICA of Bucharest,  
Splaiul Independenței no. 313, sector 1, 060042 Bucharest, Romania.  
Email: savastru\_cristina@yahoo.com

Mihaela MOREGA,  
Faculty of Electrical Engineering,  
University POLITEHNICA of Bucharest,  
Splaiul Independenței no. 313, sector 1, 060042 Bucharest, Romania.  
Email: mihaela@iem.pub.ro

